1521-0111/12/8206-1104–1114
MOLECULAR PHARMACOLOGY
U.S. Government work not protected by U.S. copyright
Mol Pharmacol 82:1104–1114, 2012

Vol. 82, No. 6
81224/3805091

Solute Restriction Reveals an Essential Role for *clag3*-Associated Channels in Malaria Parasite Nutrient Acquisition[S]

Ajay D. Pillai,[1] Wang Nguitragool,[2] Brian Lyko,[3] Keithlee Dolinta,[4] Michelle M. Butler, Son T. Nguyen, Norton P. Peet, Terry L. Bowlin, and Sanjay A. Desai

Laboratory of Malaria and Vector Research, National Institute of Allergy and Infectious Diseases, National Institutes of Health, Bethesda, Maryland (A.D.P., W.N., B.L., K.D., S.A.D.); and Microbiotix, Inc., Worcester, Massachusetts (M.M.B., S.T.N., N.P.P., T.L.B.)

Received July 13, 2012; accepted September 4, 2012

ABSTRACT

The plasmodial surface anion channel (PSAC) increases erythrocyte permeability to many solutes in malaria but has uncertain physiological significance. We used a PSAC inhibitor with different efficacies against channels from two *Plasmodium falciparum* parasite lines and found concordant effects on transport and in vitro parasite growth when external nutrient concentrations were reduced. Linkage analysis using this growth inhibition phenotype in the Dd2 × HB3 genetic cross mapped the *clag3* genomic locus, consistent with a role for two *clag3* genes in PSAC-mediated transport. Altered inhibitor efficacy, achieved through allelic exchange or expression switching between the *clag3* genes, indicated that the inhibitor kills parasites through direct action on PSAC. In a parasite unable to undergo expression switching, the inhibitor selected for ectopic homologous recombination between the *clag3* genes to increase the diversity of available channel isoforms. Broad-spectrum inhibitors, which presumably interact with conserved sites on the channel, also exhibited improved efficacy with nutrient restriction. These findings indicate that PSAC functions in nutrient acquisition for intracellular parasites. Although key questions regarding the channel and its biological role remain, antimalarial drug development targeting PSAC should be pursued.

Introduction

Malaria parasites are successful single-cell pathogens that cause immense morbidity and mortality among humans and other vertebrates. They have complex life cycles, but asexual replication within host erythrocytes is responsible for most clinical sequelae of malaria. *Plasmodium falciparum*, the most virulent human pathogen, remodels its host erythrocyte by exporting proteins (Boddey et al., 2010; Russo et al., 2010), generating membrane-bound organelles within the host cytosol (Tamez et al., 2008), and increasing erythrocyte permeability to numerous solutes (Ginsburg et al., 1983; Kirk et al., 1994).

The increased permeability is mediated by ion channels at the host erythrocyte membrane; it has been studied with tracer flux (Homewood and Neame, 1974; Saliba et al., 1998), osmotic fragility (Kutner et al., 1987), and patch-clamp (Alkhalil et al., 2004, 2012; Staines et al., 2007) techniques. Although several different channels have been proposed, studies with highly specific inhibitors support a single, broad-selectivity ion channel known as the plasmodial surface anion channel (PSAC) (Pillai et al., 2010). PSAC has an unusually small single-channel conductance for a broad-selectivity channel (20 pS in 1.1 M Cl^-) and is functionally conserved in divergent *Plasmodium* species (Lisk and Desai, 2005). Two *clag3* genes from the parasite have been impli-

This research was supported by the Medicines for Malaria Venture and the Intramural Research Program of the National Institutes of Health, National Institute of Allergy and Infectious Diseases. A.D.P. and S.A.D. are named inventors on provisional patent applications describing some of the PSAC inhibitors reported in this article. M.M.B., S.T.N., N.P.P., and T.L.B. are employees and shareholders of Microbiotix, Inc., which has obtained a license to develop PSAC inhibitors as antimalarial drugs.

A.D.P. and W.N. contributed equally to this work.

[1] Current affiliation: Wellcome Trust/DBT India Alliance, Hyderabad, India.
[2] Current affiliation: Department of Molecular Tropical Medicine and Genetics, Mahidol University, Bangkok, Thailand.
[3] Current affiliation: Towson University, Towson, Maryland.
[4] Current affiliation: University of Texas M.D. Anderson Cancer Center, Houston, Texas.

Article, publication date, and citation information can be found at http://molpharm.aspetjournals.org.
http://dx.doi.org/10.1124/mol.112.081224.

[S] The online version of this article (available at http://molpharm.aspetjournals.org) contains supplemental material.

ABBREVIATIONS: PSAC, plasmodial surface anion channel; RT, reverse transcription; PCR, polymerase chain reaction; ISPA, isolate-specific plasmodial surface anion channel antagonist; PGIM, plasmodial surface anion channel growth inhibition medium; QTL, quantitative trait locus; MTS, 3-(4,5-dimethylthiazol-2-yl)- 5-(3-carboxymethonyphenol)-2-(4-sulfophenyl)-2*H*-tetrazolium, inner salt.

cated in this channel activity through a molecular cloning strategy using an inhibitor that blocks channels from only the Dd2 parasite line (isolate-specific PSAC antagonist 28, ISPA-28) (Nguitragool et al., 2011).

Although direct evidence is lacking, circumstantial observations suggest that PSAC activity is essential for intraerythrocytic parasite survival. First, both channel activity and the *clag* gene family are conserved in all *Plasmodium* species examined to date (Kaneko et al., 2001; Lisk and Desai, 2005). Single-channel patch-clamp studies determined that even biophysical properties such as ion channel gating, conductance, and functional copy number per cell are nearly identical in *P. falciparum* and *Plasmodium knowlesi*, two divergent malaria parasites (Lisk and Desai, 2005). Second, gene silencing and monoallelic expression of *clag3* genes in *P. falciparum* suggest that channel function is important (Cortés et al., 2007); parasites invest in expression switching for key gene families to evade host immunity and to protect essential activities at the host cell surface (Scherf et al., 2008). Third, quantitative permeability studies with some required nutrients suggested that their PSAC-mediated uptake is necessary for in vitro parasite cultivation (Gero and Wood, 1991; Saliba et al., 1998; Liu et al., 2006; Martin and Kirk, 2007). Finally, selections of parasite cultures with permeant toxins has generated functional PSAC mutants (Hill et al., 2007; Lisk et al., 2008) but has not yielded complete loss of function. These mutant channels exhibit reduced toxin uptake but appear to satisfy the parasite's transport demands. It remains possible, however, that channel activity is a nonessential byproduct of host cell invasion (Staines et al., 2007). The physiological roles served by PSAC are also debated, with proposals including nutrient uptake and metabolic waste removal (Desai et al., 2000), modification of host erythrocyte ionic composition (Brand et al., 2003), volume regulation of infected cells (Staines et al., 2001; Lew et al., 2004), and autocrine purinergic signaling (Akkaya et al., 2009).

We addressed these uncertainties with functional and molecular studies using ISPA-28. This and other PSAC inhibitors exhibit improved efficacy in parasite growth inhibition studies when the concentrations of key nutrients are reduced. Genetic mapping, DNA transfection, and in vitro selections implicate the *clag3* genes in channel-mediated nutrient uptake required for parasite survival within erythrocytes.

Materials and Methods

Parasite Cultivation, Design of PGIM, and Growth Inhibition Studies. Asexual-stage *P. falciparum* laboratory lines were propagated with standard methods, in RPMI 1640 medium supplemented with 25 mM HEPES, 31 mM $NaHCO_3$, 0.37 mM hypoxanthine, 10 μg/ml gentamicin, and 10% pooled human serum. Nutrient-deprivation experiments used this standard medium but with reduced concentrations of individual constituents; human serum was exhaustively dialyzed against distilled water before addition to those media. PGIM contained reduced concentrations of isoleucine (11.4 μM), glutamine (102 μM), and hypoxanthine (3.01 μM) and was supplemented with dialyzed serum.

The results of growth inhibition experiments were quantified by using a SYBR Green I-based fluorescence assay for parasite nucleic acid in 96-well microplates, as described previously (Pillai et al., 2010). Ring-stage synchronized cultures were seeded at 1% parasitemia and 2% hematocrit levels in standard medium or PGIM and were maintained for 72 h at 37°C in 5% O_2/5% CO_2 in nitrogen, without medium changes. Cultures were then lysed in 20 mM Tris, 10 mM EDTA, 0.016% saponin, 1.6% Triton X-100, pH 7.5, with SYBR Green I nucleic acid gel stain (Invitrogen, Carlsbad, CA) at 5000-fold dilution. After a 45-min incubation, parasite DNA contents were quantified through fluorescence measurements (excitation, 485 nm; emission, 528 nm). For each inhibitor concentration, the mean of triplicate measurements was calculated after subtraction of background fluorescence values determined with matched cultures that had been killed with 20 μM chloroquine. Growth inhibition studies with the $HB3^{3rec}$ parasite were performed after transport-based selection with ISPA-28, to achieve expression of the chimeric *clag3* gene generated through allelic exchange transfection. Limiting-dilution cultures to obtain parasite clones were performed in 96-well microplates; positive wells were detected by using the 5(and 6)-carboxy-seminaphthorhodafluor-1 method (Lyko et al., 2012).

Parasites were also cultivated in pooled human serum collected from nonfasting donors (Interstate Blood Bank, Memphis, TN). The serum was ultracentrifuged (300,000*g* for 1 h) to remove buoyant lipoproteins and was used in 72-h cultivation experiments in microplates as described above. Growth was quantified as described above except that microplate wells were washed once with phosphate-buffered saline before the addition of buffered SYBR Green I gel stain, to eliminate serum-associated fluorescence artifacts.

Transport-Inhibition Assays. Inhibitor affinity for PSAC block was determined by using a quantitative transmittance assay based on the osmotic lysis of infected cells with sorbitol (Pillai et al., 2010). Parasite cultures were enriched at the trophozoite stage with the Percoll-sorbitol method, washed, and resuspended at 37°C and 0.15% hematocrit in 280 mM sorbitol, 20 mM Na-HEPES, 0.1 mg/ml bovine serum albumin, pH 7.4, with the indicated inhibitor concentrations. Osmotic lysis, which results from PSAC-mediated sorbitol uptake, was continuously tracked with transmittance measurements through the cell suspension (700-nm wavelength, DU640 spectrophotometer with Peltier temperature control; Beckman Coulter, Fullerton, CA). Inhibitor dose-response relationships were calculated from the times required to reach a fractional lysis threshold. ISPA-28 dose-response data were fitted to the sum of two Langmuir isotherms with the following equation: $P = a/[1 + (x/b)] + (1 - a)/[1 + (x/c)]$, where P represents the normalized sorbitol permeability in the presence of inhibitor at concentration x, and a, b, and c are constants. Dose-response data for other inhibitors were fitted adequately with a single Langmuir isotherm.

To examine possible inhibitor metabolism in parasite cultures, we cultivated Dd2 parasites for 72 h at 37°C in standard medium with 40 μM ISPA-28. After centrifugation, the culture supernatant was used as a source of ISPA-28 for comparison with freshly prepared compound in transport-inhibition studies.

QTL Analyses. We sought genetic loci associated with ISPA-28 growth-inhibitory efficacy in the Dd2 × HB3 genetic cross (Wellems et al., 1990) by using 448 previously selected polymorphic markers that distinguish the Dd2 and HB3 parental lines (Nguitragool et al., 2011). QTL analysis was performed with R/qtl software (freely available at http://www.rqtl.org/) as described (Broman et al., 2003), with conditions suitable for the haploid asexual parasite. A significance threshold of $P = 0.5$ was estimated through permutation analysis. Growth inhibition data at 0.3 and 10 μM ISPA-28 identified the same locus described with 3 μM ISPA-28. Additional QTLs were sought with secondary scans controlling for the *clag3* locus.

Quantitative RT-PCR Assays. Two-step, real-time, PCR assays with allele-specific primers developed previously (Nguitragool et al., 2011) were used to quantify *clag* gene expression. RNA was harvested from schizont-stage cultures with TRIzol reagent (Invitrogen), treated with DNase, and used for reverse transcription with oligo(dT) primers and SuperScriptIII (Invitrogen). Negative control reactions without reverse transcriptase confirmed that there was no genomic DNA contamination. Real-time PCR assays were performed

with a QuantiTect SYBR Green PCR kit (QIAGEN, Valencia, CA), an iCycler iQ multicolor, real-time, PCR system (Bio-Rad Laboratories, Hercules, CA), and *clag* gene-specific primers (Supplemental Table 1). Serial dilutions of parasite genomic DNA were used to construct the standard curve for each primer pair. PF7_0073 was used as a loading control, because it is expressed constitutively. Transcript abundance for each *clag* gene was determined from amplification kinetic data.

PCR Studies of *clag3* Recombination. The *clag3* locus of Dd2-*PGIM28* was characterized with genomic DNA and the following allele-specific primers: *3.1f*, 5′-GTGCAATATATCAAAGTGTACATGCA-3′; *3.1r*, 5′-AAGAAAATAAATGCAAAACAAGTTAGA-3′; *3.2f*, 5′-GTTGAGTACGCACTAATATGTCAATTTG-3′; *3.2r*, 5′-AACCATAACATTATCATATATGTTAATTACAC-3′. cDNA prepared from schizont-stage cultures was used with these primers to examine the expression of both native and chimeric *clag3* genes.

Southern Blotting. A *clag3*-specific probe was prepared from Dd2 genomic DNA through PCR amplification with 5′-ATTTACAAACAAAGAAGCTCAAGAGGA-3′ and 5′-TTTTCTATATCTTCATTTTCTTTAATTGTTC-3′ in the presence of digoxygenin-dUTP (Roche Diagnostics, Basel, Switzerland). Probe specificity was confirmed through blotting against full-length PCR amplicons of the five *clag* genes generated from Dd2 genomic DNA with the primers listed in Supplemental Table 2.

Genomic DNA was digested with the indicated restriction enzymes (New England BioLabs, Ipswich, MA), subjected to electrophoresis in 0.7% agarose gels, acid-depurinated, transferred, and crosslinked to nylon membranes. The blots were then hybridized overnight at 39°C with the aforementioned digoxygenin-labeled probe in DIG Easy Hyb solution (Roche Diagnostics) and were washed with low- and high-stringency buffers (2× saline-sodium citrate 0.1% SDS, at 23°C, followed by 1× saline-sodium citrate, 0.5% SDS, at 50°C) before digoxygenin immunodetection according to the manufacturer's instructions.

Mammalian Cytotoxicity Assays. Inhibitor cytotoxicity was quantified by using human HeLa cells (CLL-2; American Type Culture Collection, Manassas, VA) seeded at 4000 cells/well in 96-well plates. Cultures were incubated with individual inhibitors for 72 h at 37°C in minimal essential medium (Invitrogen) supplemented with 10% fetal calf serum. Cell viability was quantified by using the vital stain 3-(4,5-dimethylthiazol-2-yl)-5-(3-carboxymethonyphenol)-2-(4-sulfophenyl)-2*H*-tetrazolium, inner salt (MTS), as described (Marshall et al., 1995).

Results

Poor Growth Inhibition by ISPA-28 under Standard Culture Conditions. ISPA-28 blocks PSAC on Dd2-infected cells with high affinity and has only weak activity against channels from HB3 parasites ($K_{0.5}$ values of 56 ± 5 nM and 43 ± 2 μM, respectively) (Nguitragool et al., 2011). If channel activity serves an essential role, then this small-molecule inhibitor should interfere with the propagation of Dd2 cultures but not HB3 cultures. Our initial in vitro parasite growth studies revealed an insignificant difference, with both parasite lines exhibiting sustained growth in RPMI 1640 medium despite high ISPA-28 concentrations (IC_{50} values of >40 μM for both lines) (data not shown).

We considered possible explanations and determined that ISPA-28 efficacy against Dd2 channels was not compromised by metabolism of the inhibitor under in vitro culture conditions (Supplemental Fig. 1A). ISPA-28 was not significantly adsorbed by serum proteins or lipids (Supplemental Fig. 1, B–D), a phenomenon that is known to reduce the activity of some PSAC inhibitors and many therapeutic agents (Matsuhisa et al., 1987). Therefore, ISPA-28 has unexpectedly poor efficacy against the growth of Dd2 parasites.

One possibility is that channel activity is essential for malaria parasites but low transport levels remaining in the presence of inhibitor adequately meet parasite demands under standard in vitro culture conditions. Consistent with this idea, we noted sustained channel-mediated uptake in Dd2-infected erythrocytes even with high ISPA-28 concentrations; significantly less residual uptake was observed with compound **2**, a broad-spectrum PSAC inhibitor with a comparable inhibitory $K_{0.5}$ value for Dd2 channels ($P < 10^{-4}$ for comparison of these inhibitors at 10 μM) (Supplemental Fig. 2). The unexpected difference in residual channel activities with these inhibitors may account for their different efficacies against in vitro parasite growth (IC_{50} values of >40 and 4.7 μM, respectively) (Table 1).

Incomplete block with high ISPA-28 concentrations despite a low $K_{0.5}$ value for Dd2 channels suggests a complex mechanism of inhibition. Although dantrolene and furosemide dose-response data were adequately fitted with an equation that assumed 1:1 stoichiometry for inhibitor and channel molecules (Langmuir isotherm) (Supplemental Fig. 1, C and D), the ISPA-28 dose-response data were not well fitted (Supplemental Fig. 2). An improved fit was obtained with a two-component Langmuir equation. Because this two-component equation is consistent with several possible mechanisms, the stoichiometry and precise mode of channel block with ISPA-28 remain unknown.

Selective Inhibition of Dd2 Growth by ISPA-28 When Nutrients Are Restricted. If PSAC functions in nutrient acquisition for the intracellular parasite (Desai et al., 2000), then the incomplete inhibition by ISPA-28 may permit adequate nutrient uptake. This effect may be accentuated in cultures using RPMI 1640 medium, which contains high nutrient concentrations to support the growth of diverse cell lines (Sato and Kan, 2001). The large inward concentration gradients for nutrients in this medium may sustain parasite nutrient uptake despite nearly complete channel block.

To evaluate this possibility, we examined parasite requirements for isoleucine, an essential amino acid that the parasite cannot synthesize de novo (Istvan et al., 2011). Isoleucine is absent from human hemoglobin, which the parasite digests as a source of some amino acids; it must be acquired through uptake from serum (Liu et al., 2006; Martin and Kirk, 2007). We prepared RPMI 1640 media with a range of isoleucine concentrations and determined that Dd2 and HB3 parasites had quantitatively similar isoleucine requirements, with negligible growth when this amino acid is removed from the medium (EC_{50} values of 10–16 μM isoleucine) (Fig. 1A). The addition of 15 μM ISPA-28 significantly increased Dd2 requirement for isoleucine (EC_{50} = 34.6 ± 1.1 μM; $P < 10^{-9}$, Student's *t* test) but had no effect on HB3 parasites. This finding suggests an essential role for PSAC-mediated isoleucine uptake and is consistent with transport studies that showed this channel to be a major route of uptake after infection.

Because many nutritive solutes have significant PSAC permeability, we also examined parasite growth in RPMI 1640 medium after isolated removal of several other solutes, i.e., calcium panthothenate, cysteine, glutamic acid, glutamine, methionine, proline, and tyrosine. Hypoxanthine, a purine source that is not present in RPMI 1640 medium but is commonly added to parasite culture media, was also evaluated. Each of these solutes has documented PSAC permea-

TABLE 1
Effects of broad-spectrum PSAC inhibitors and antimalarial drugs that act at other sites

Compound	Structure	$K_{0.5}$ for PSAC Block	IC_{50} for Growth Inhibition		IC_{50} Ratio
			RPMI 1640 Medium	PGIM	
		nM	*μM*		
ISPA-28	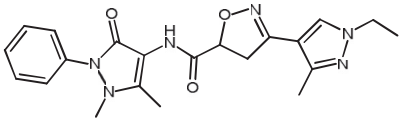	Dd2, 56; HB3, 43,000	Dd2, >40; HB3, >40	Dd2, 0.66; HB3, >50	Dd2, >60; HB3, N.D.
Furosemide	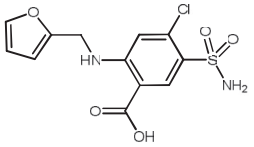	2700	>200	21	>9.5
Dantrolene	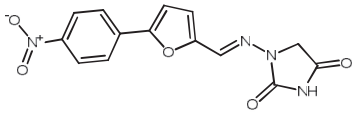	1200	42	3.8	18
1	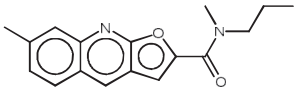	87	23	0.27	114
3	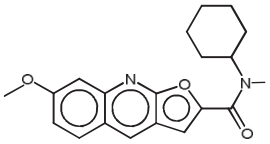	33	15	0.17	86
9	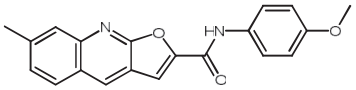	6	18	0.23	270
2	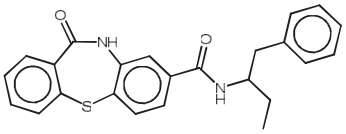	84	4.7	0.41	15
TP-52	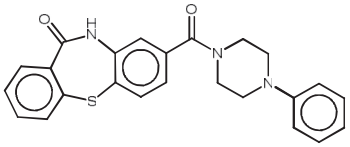	25	7.3	0.19	38
8	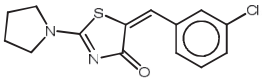	44	12.5	0.17	130
5	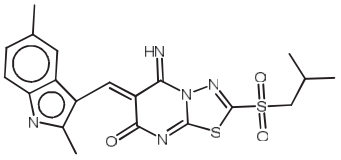	81	>30	2.0	>15
ISG-21	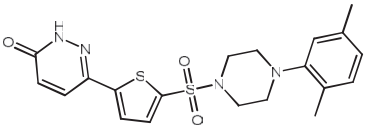	2.6	1.5	0.002	800
Chloroquine		Inactive	0.22	0.34	0.67
Mefloquine		Inactive	0.022	0.033	0.66
Artemisinin		Inactive	0.018	0.026	0.66

N.D., not determined.

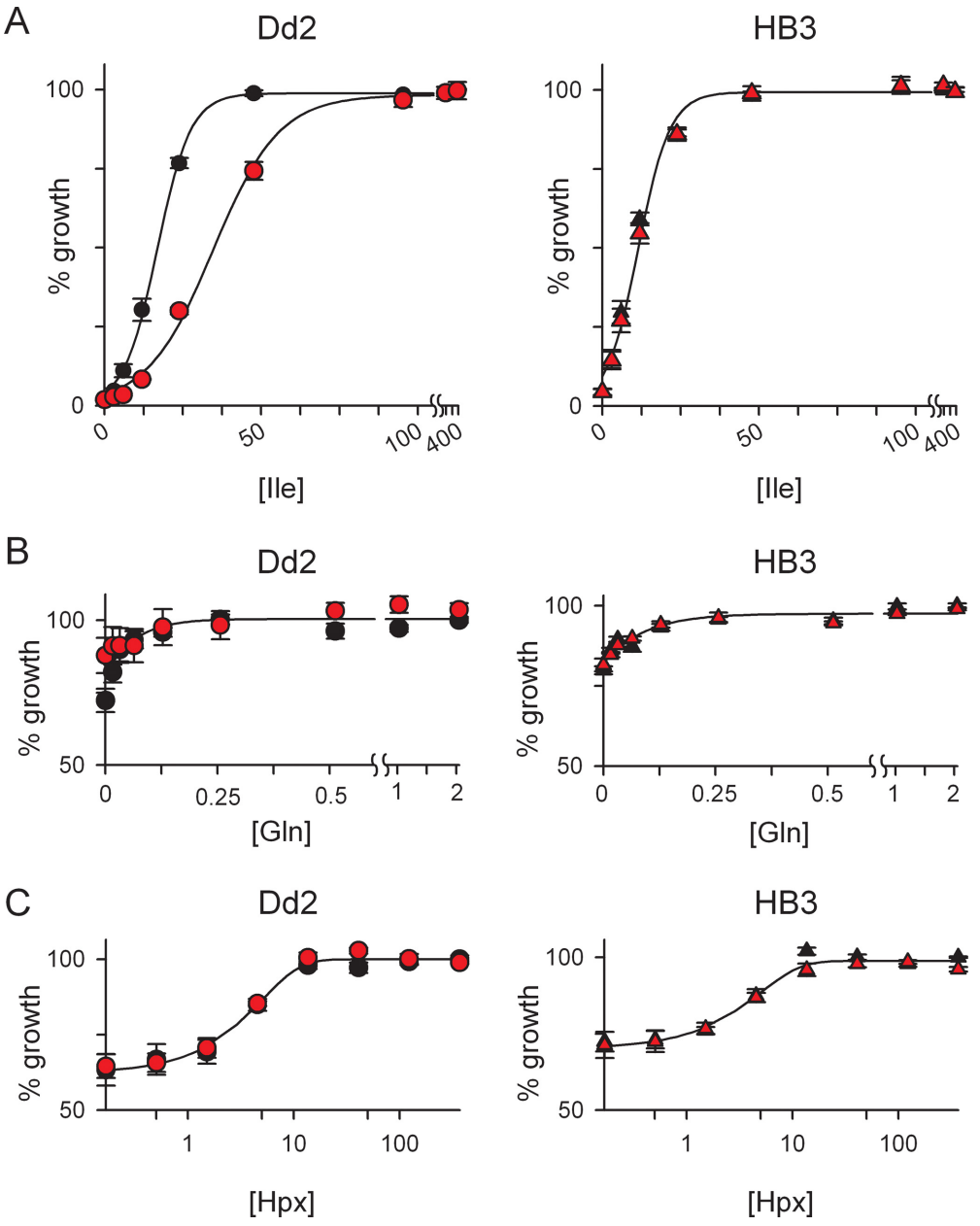

Fig. 1. Dose-response curves for parasite nutrient requirements and effects of ISPA-28. Normalized parasite growth rates over 72 h in standard RPMI 1640 medium with the indicated depletions of isoleucine (A), glutamine (B), or hypoxanthine (C) are shown; all media were supplemented with 10% dialyzed human serum. Left, Dd2 parasites; right, HB3 parasites. Symbols represent mean ± S.E.M. of six to nine trials from up to three independent experiments. Black symbols, experiments without addition of ISPA-28; red symbols, experiments with addition of 15 μM ISPA-28. Solid lines, best fits of the data to sigmoidal growth curves. ISPA-28 significantly increased Dd2 demand for isoleucine but had no effect on that of HB3 parasites.

bility (Ginsburg et al., 1985; Gero and Wood, 1991; Asahi et al., 1996; Saliba et al., 1998; Lisk et al., 2006), but some also exhibit uptake by host erythrocyte transporters (Quashie et al., 2010; Winterberg et al., 2012). Microscopic examination of parasites propagated in these single-depletion experiments revealed the greatest detriment with removal of glutamine and hypoxanthine, but short-term growth studies revealed relatively modest effects (Fig. 1, B and C). The addition of ISPA-28 did not measurably increase Dd2 requirement for either solute in these experiments.

Because parasite growth reflects a complex interplay of multiple biochemical pathways and the availability of nutrients that feed into them, the effects of PSAC inhibition may be greater than predicted by deprivation studies restricted to single solutes. Therefore, we simultaneously varied the concentrations of isoleucine, glutamine, and hypoxanthine without manipulating other constituents in the RPMI 1640 medium. This approach revealed conditions that increased ISPA-28 potency against Dd2 parasites while preserving the negligible effect of the compound against HB3 parasites (Fig. 2A).

In the absence of transport inhibitors, this medium, termed PGIM, permitted continuous propagation of both Dd2 and HB3 parasites for >2 weeks, although at somewhat reduced rates (Fig. 2B). We noticed that cultures with low parasitemia levels grew well in PGIM but rates decreased with greater parasite burdens, which is consistent with nutrient limitation and competition among parasites in culture. To explore how these conditions might compare with in vivo expansion rates, we examined parasite propagation in pooled nonfasting serum collected from healthy donors. Human serum that was not diluted with synthetic medium also yielded relatively slow expansion of parasite cultures (Fig. 2B), which is consistent with the view that RPMI 1640 medium achieves high culture expansion rates through the use of supraphysiological nutrient levels.

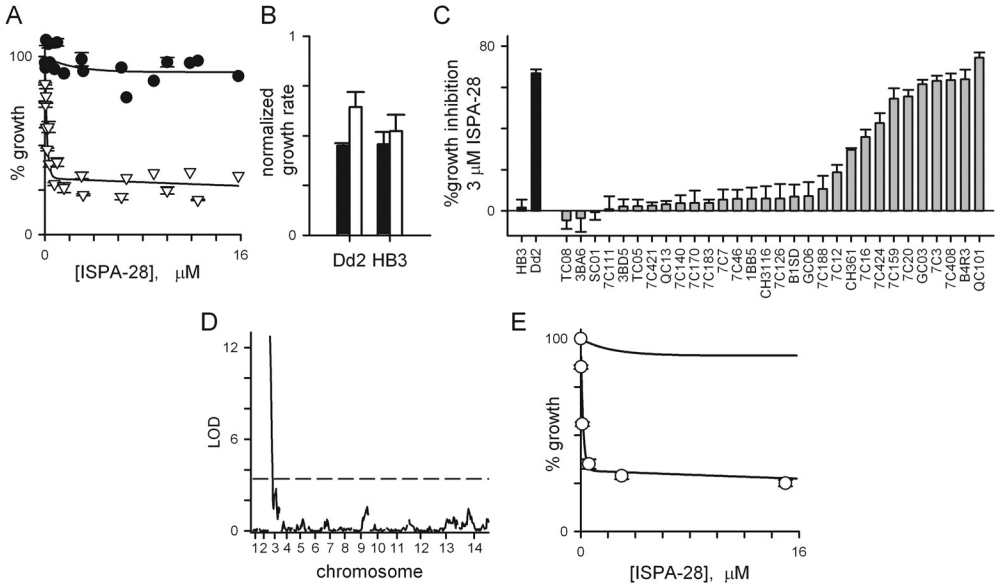

Fig. 2. ISPA-28 inhibition of parasite growth through direct action on *clag3*-associated channels. A, parasite growth rates in PGIM as a function of ISPA-28 concentration. ISPA-28 inhibited Dd2 growth (▽) but not HB3 growth (●). Solid lines, best fits to a two-component, exponential-decay function. B, growth rates (mean ± S.E.M.) over 72 h in PGIM (■) or pooled human serum (□), each normalized to 1 for matched cultures in RPMI 1640 medium. C, growth inhibition (mean ± S.E.M.) by 3 μM ISPA-28 for the indicated parental lines and progeny clones. Most progeny exhibited ISPA-28 sensitivity resembling one or the other parent. D, associated logarithm of odds (LOD) scores from a primary QTL scan. The peak score mapped to the *clag3* locus on parasite chromosome 3. Dashed line, $P = 0.05$ significance threshold calculated from 1000 permutations. E, ISPA-28 dose-response curve for growth inhibition of HB3^{3rec} in PGIM. Solid lines, ISPA-28 sensitivities of HB3 and Dd2 parasites (data from A).

Linkage Analyses and DNA Transfection Studies. Although the ISPA-28 IC_{50} values for growth in PGIM (0.66 ± 0.20 and 52 ± 19 μM for Dd2 and HB3 parasites, respectively; $P < 10^{-4}$) agree reasonably well with the $K_{0.5}$ values for transport inhibition, differing efficacies against parasite growth might also reflect effects of the inhibitor on other parasite targets. Therefore, we examined the ISPA-28 growth inhibition phenotype in the progeny of the Dd2 × HB3 genetic cross (Wellems et al., 1990). These studies revealed a broad range of ISPA-28 efficacies for progeny clones (Fig. 2C), with many progeny resembling one or the other parent. Because HB3 parasites and some progeny had high growth IC_{50} values that could not be determined precisely, linkage analysis was performed by using growth inhibition with 3 μM ISPA-28, a concentration that optimally distinguishes the parental phenotypes. The analysis identified a single parasite genomic locus at the 5′-end of chromosome 3 with high confidence (logarithm of odds score of 12.7) (Fig. 2D). Additional contributing genomic loci were sought after removing the effects of this locus but were not identified in secondary scans (Supplemental Fig. 3).

The mapped locus contains many genes but most notably the two *clag3* genes that were recently implicated in PSAC activity. To determine whether the proteins encoded by these genes are the growth-inhibitory targets of ISPA-28, we performed studies with HB3^{3rec}, a parasite clone generated through allelic exchange transfection of HB3 to replace the 3′-end of the native *clag3.2* gene with the corresponding fragment of the Dd2 *clag3.1* gene. When this chimeric gene was expressed, HB3^{3rec} parasites exhibited high-affinity inhibition by ISPA-28 ($K_{0.5}$ = 51 ± 9 nM; $P = 0.88$ for no difference from Dd2 value) (Nguitragool et al., 2011). In PGIM-based growth inhibition studies, HB3^{3rec} parasites were highly sensitive to ISPA-28 at levels that matched those for Dd2 parasites (Fig. 2E), which indicates that ISPA-28 toxicity is mediated through action on the *clag3* product. Moreover, the need for nutrient restriction to detect the growth-inhibitory effects of this compound supports a primary role for PSAC in parasite nutrient acquisition.

Selective Growth of Parasites with Resistant *clag3* Alleles. We explored the role of the channel further by evaluating whether PSAC inhibitors and PGIM could be used to kill selectively parasites that express individual *clag3* genes. Most laboratory parasite lines carry two *clag3* genes on chromosome 3, but individual parasites appear to express only one allele at a time (Fig. 3A). Silencing of the other allele is thought to occur through epigenetic mechanisms (Cortés et al., 2007). This process, with relatively slow rates of switching between the two alleles, allows subsets of parasites to escape host immune responses against surface-exposed antigens.

ISPA-28 specifically inhibits channels associated with the Dd2 *clag3.1* gene because it binds to a region near the C terminus of the encoded protein; it has little or no activity against channels linked to expression of Dd2 *clag3.2* or either *clag3* gene in unrelated parasite lines (Nguitragool et al., 2011). This inhibitor was used previously to select for Dd2 *clag3.1* expression through osmotic lysis of infected cells with sorbitol, a sugar alcohol with high PSAC permeability. Sorbitol solutions containing ISPA-28 select for this allele because osmotic lysis eliminates infected cells whose channels are not blocked (Fig. 3B).

We hypothesized that ISPA-28 and PGIM might be useful in counter-selections for other *clag3* alleles (Fig. 3B). Whereas sorbitol-induced osmotic lysis selects for expression of the ISPA-28-sensitive *clag3.1* gene, growth inhibition in PGIM should favor cells expressing the resistant *clag3.2* allele, because only parasites expressing unblocked channels could meet their nutrient demands and propagate successfully. We first examined the progeny clone 7C20, which carries the Dd2 *clag3* locus and expresses both alleles in unselected cultures (Fig. 3, C–E). After selection through osmotic lysis with sorbitol and ISPA-28, surviving parasites had PSAC inhibitor affinities that matched those of the Dd2 parent; these parasites expressed predominantly the *clag3.1* allele. The culture was then propagated for a total of 10 days in PGIM containing 5 μM ISPA-28; microscopic examination of smears obtained during this treatment revealed nearly complete sterilization of the culture. Channels expressed by parasites that survived this second treatment had markedly reduced ISPA-28 affinity, which indicates that in vitro propagation with PSAC inhibitors can be used to select for rare

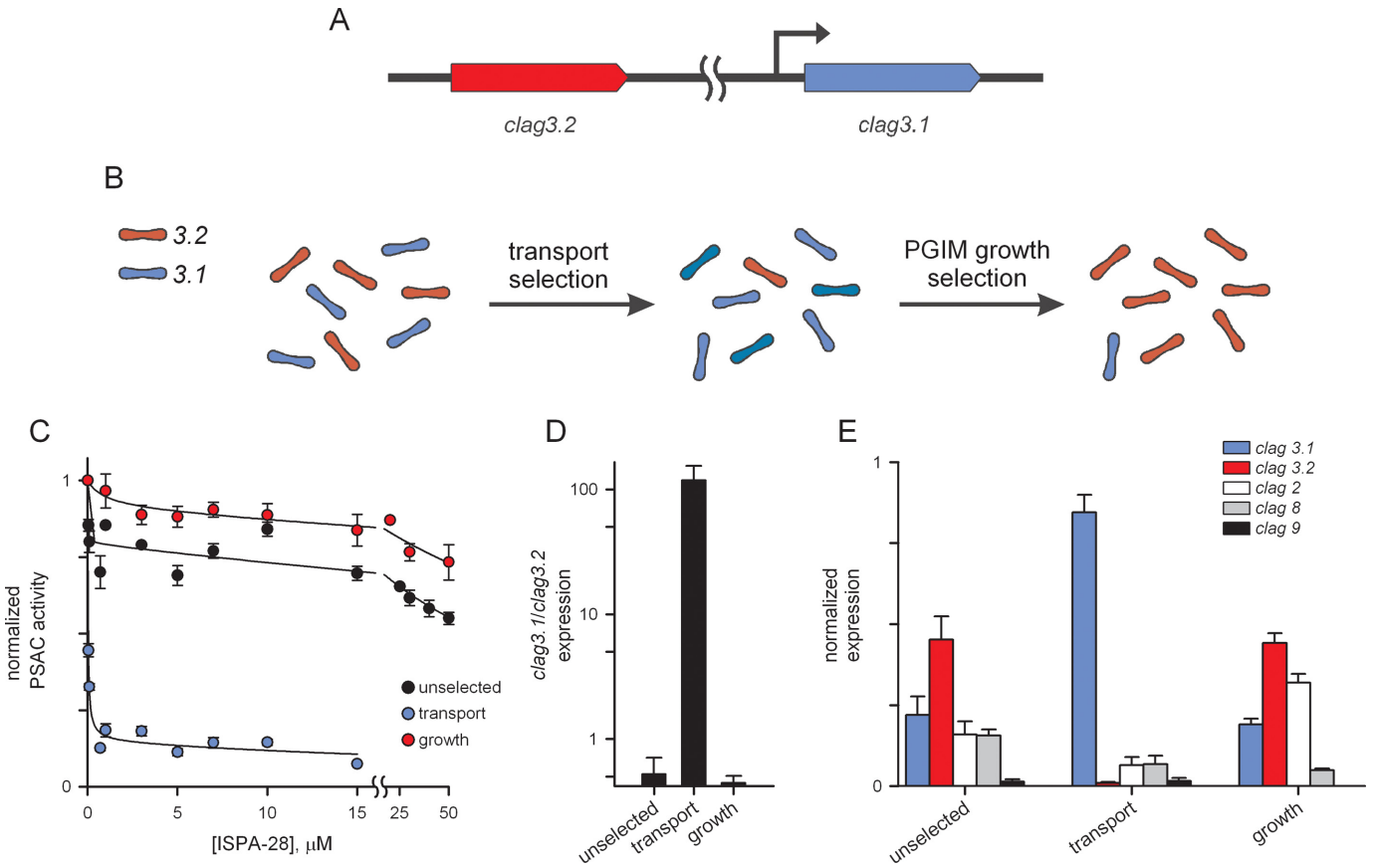

Fig. 3. In vitro growth selection for *clag3* alleles associated with inhibitor-resistant channels. A, schematic diagram showing the two *clag3* genes of the 7C20 progeny clone. Arrow, active transcription of *clag3.1*. B, strategy for purifying selections for *clag3.1* (blue) or *clag3.2* (red) expression. Osmotic lysis of 7C20-infected cells with sorbitol and ISPA-28 spared cells that expressed *clag3.1* (transport selection), whereas PGIM-based growth inhibition by ISPA-28 selected for *clag3.2* expression. C, ISPA-28 dose-response curves (mean ± S.E.M.) for PSAC inhibition before selection, after transport selection of the 7C20 line, and after PGIM growth selection. Solid lines, best fits to the equation provided in *Materials and Methods*. D, expression ratios for the two *clag3* alleles before and after selections, as determined with quantitative RT-PCR assays. High-affinity ISPA-28 block was associated with *clag3.1* expression. Bars, mean ± S.E.M. of replicates from two to four separate trials each. E, expression (mean ± S.E.M.) of the five *clag* genes before and after each selection.

parasite subpopulations. Consistent with our predictions, RT-PCR assays confirmed strong negative selection against *clag3.1*, to yield parasites that preferentially expressed *clag3.2*. There were modest changes in the expression of *clag* genes on other chromosomes, which suggests that those paralogs may also contribute to PSAC activity. Importantly, the opposing effects of ISPA-28 on in vitro growth inhibition and on susceptibility to transport-induced osmotic lysis permitted purifying selections of either *clag3* allele and revealed a strict correlation with channel phenotype.

Genomic Recombination to Overcome Defect in Epigenetic Switching. The parental Dd2 line retains exclusive expression of *clag3.1* in unselected cultures, despite being isogenic with 7C20 at the *clag3* locus. To explore possible mechanisms, we sought to select for Dd2 parasites expressing the *clag3.2* allele. We first attempted transport selection using osmotic lysis with isolate-specific PSAC antagonist 43 (Supplemental Fig. 4A), an unrelated PSAC inhibitor with higher affinity for channels formed by expression of Dd2 *clag3.2* than of *clag3.1*. Although this approach was used previously to select for 7C20 parasites expressing *clag3.2* (Nguitragool et al., 2011), it proved insufficient to affect the channel phenotype in Dd2 parasites, despite repeated selections over 4 months (Supplemental Fig. 4, B and C).

We next attempted negative selection with growth inhibition in PGIM containing ISPA-28. After two cycles of drug pressure with 5 μM ISPA-28 for a total of 17 days, resistant cells were identified and characterized after limiting dilution to obtain the clone Dd2-*PGIM28*. Consistent with killing primarily through PSAC inhibition, transport studies with this resistant clone revealed a marked reduction in inhibitor affinity (Fig. 4A). Surprisingly, although the ISPA-28 dose-response relationship quantitatively matched that of 7C20 parasites after identical PGIM-based selection (Fig. 4A), full-length *clag3.2* transcript was still undetectable (Fig. 4B). Because this observation excludes simple gene-switching, we considered spontaneous recombination between the two *clag3* genes. We identified a chimeric *clag3* transcript by using a forward *clag3.1* primer and a reverse *clag3.2* primer; PCR analyses confirmed that this chimera is present in the genome of the selected parasites but absent from the original Dd2 line (Fig. 4C). Southern blotting with a *clag3*-specific probe detected three discrete bands in the selected clone but only the expected two bands in unselected Dd2 parasites (Fig. 4D; Supplemental Fig. 5), implicating a recombination event to produce three *clag3* genes in Dd2-*PGIM28* (Fig. 4E). The size of the new band, ~16 kb, matches the intergenic distance between *clag3.1* and *clag3.2* and is consistent with homologous recombination in Dd2-*PGIM28*. DNA sequencing

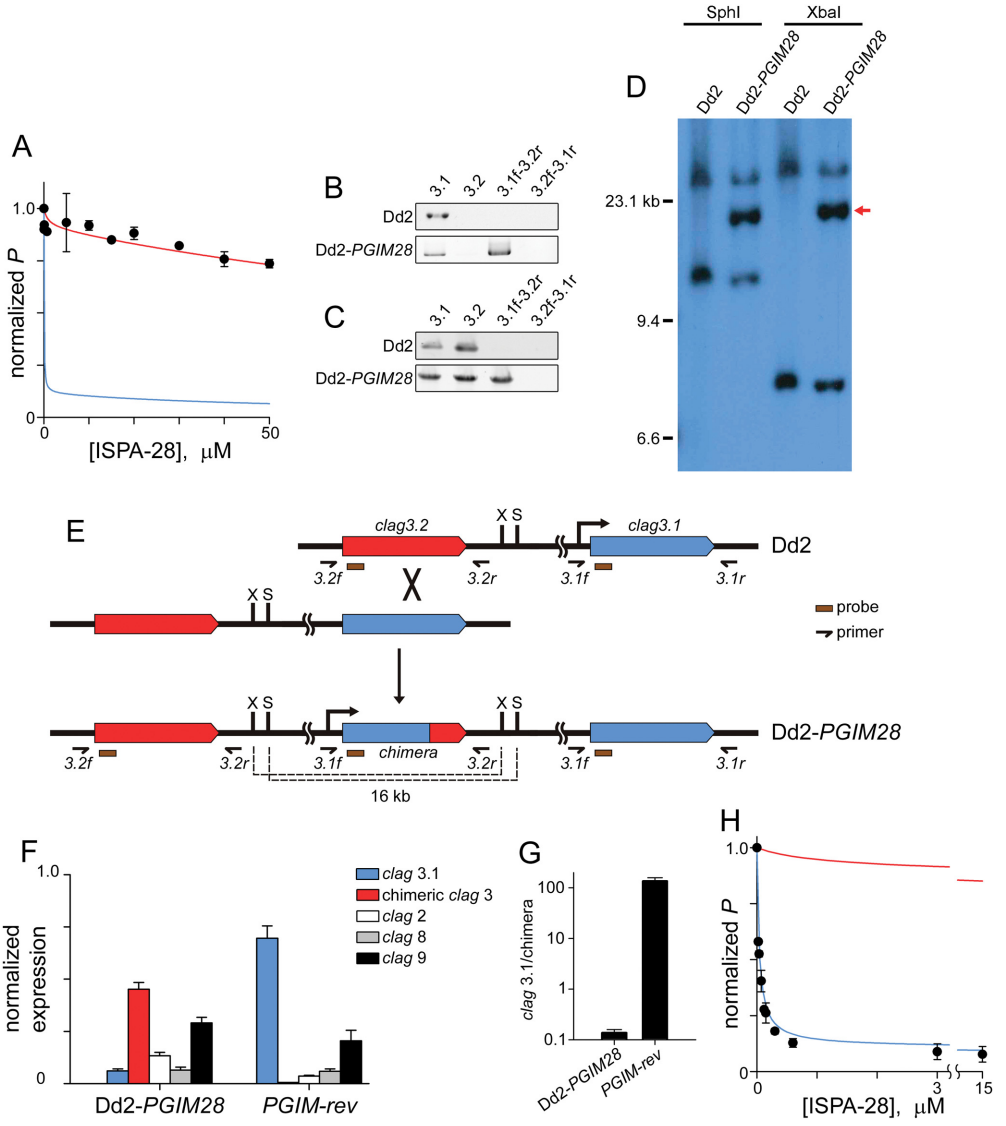

Fig. 4. Ectopic recombination of *clag3* genes in Dd2 parasites under selective pressure. A, ISPA-28 dose-response curve for PSAC inhibition in the Dd2-*PGIM28* line (circles) (mean ± S.E.M. of up to five measurements each). Solid lines, dose-response curves for *clag3.1* (blue) and *clag3.2* (red) expression in 7C20 (from Fig. 3C). B, ethidium bromide-stained gels showing RT-PCR amplicons for expression of native *clag3* genes (*3.1* and *3.2*) or chimeric genes resulting from recombination (*3.1f-3.2r* and *3.2f-3.1r*). C, PCR amplicons for native and chimeric *clag3* gene permutations from genomic DNA of the indicated parasites. Dd2-*PGIM28* carries and expresses a chimeric gene (*3.1f-3.2r*). D, Southern blot showing three *clag3* copies in the Dd2-*PGIM28* parasite but only two in the original Dd2 line. DNA samples were digested with SphI or XbaI, and a *clag3*-specific probe was used for detection. The size of the additional band in Dd2-*PGIM28* (16 kilobases) (red arrow) is consistent with homologous recombination between the two *clag3* genes. E, schematic diagram showing homologous recombination between the native *clag3* genes of Dd2 to produce three copies in Dd2-*PGIM28*. The site of recombination, indicated by a blue-to-red transition in the chimeric gene, was determined through DNA sequencing. The sites recognized by primers (in B and C) and the probe used for Southern blotting (in D) are indicated; vertical lines marked X and S represent XbaI and SphI restriction sites, respectively, as used in Southern blotting. F, expression (mean ± S.E.M.) of each *clag* gene in *Dd2-PGIM28* before and after transport-based selection for *clag3.1* with ISPA-28 (*PGIM-rev*). G, ratios quantifying the relative expression of *clag3* and the chimeric gene, calculated from data in F and presented on a logarithmic scale. H, PSAC inhibition by ISPA-28 in the *PGIM-rev* line. Solid lines, from Fig. 3C.

indicated that the chimeric gene derives its 5′-untranslated region and the first ~70% of the gene from *clag3.1*. After crossover between single-nucleotide polymorphisms 3680 and 3965 base pairs from the start codon, the gene carries the 3′-end of *clag3.2*. Therefore, the chimeric gene is driven by the *clag3.1* promoter but encodes a protein with the C-terminal variable domain of *clag3.2*. This altered C terminus accounts for the reduced ISPA-28 efficacy against nutrient uptake and thus the survival of this clone in our selection. Such homologous recombination also produces a parasite with a single *clag3* gene and high ISPA-28 affinity, but that recombinant is not expected to survive growth inhibition selection in PGIM with ISPA-28.

We used quantitative RT-PCR assays to examine the transcription of *clag* genes in Dd2-*PGIM28* and found that the chimeric gene is preferentially expressed (8.9 ± 1.3-fold greater than *clag3.1*; $P < 0.002$) (Fig. 4F). We then performed transport-based selection with sorbitol and ISPA-28 to examine whether Dd2-*PGIM28* can undergo expression switching. As expected for an intact *clag3.1* promoter and gene, this second selection yielded parasites that expressed native *clag3.1* almost exclusively (*PGIM-rev*) (Fig. 4, F and G). Transport studies revealed an ISPA-28 dose-response relationship identical to that of the original Dd2 line (Fig. 4H). Therefore, the new chimeric *clag3* gene can undergo epigenetic silencing and switching with *clag3.1*. It is not clear why the native *clag3.2* gene of Dd2 parasites is refractory to transcription: DNA sequencing of the gene's promoter region did not reveal any mutations relative to that of 7C20.

These findings indicate that recombination between the two *clag3* genes occurs with relative ease, consistent with reports of frequent recombination events in the parasite's subtelomeric regions (Freitas-Junior et al., 2000). Such recombination events may serve to increase diversity in PSAC phenotypes, which is apparent here as affording survival of a parasite with three *clag3* genes under selective pressure.

Conserved PSAC Inhibitors and Antimalarial Drugs that Act at Other Targets. To examine further the physiological role of PSAC, we compared the growth-inhibitory effects of other PSAC inhibitors in PGIM and standard medium (Table 1). Furosemide and dantrolene are known nonspecific inhibitors with relatively low PSAC affinity. These compounds are adsorbed by serum (Supplemental Fig. 1, C and D) but are approved therapeutic agents for other human

diseases. They were only weakly effective against parasite growth in standard medium, but they exhibited significantly improved activity in PGIM. We also tested eight high-affinity PSAC inhibitors from five distinct scaffolds that were identified through high-throughput screening (Pillai et al., 2010). Each of the inhibitors was more potent when nutrient concentrations were reduced, strengthening the evidence for the channel's role in nutrient acquisition. The extent of improved efficacy was variable, but many compounds exhibited >100-fold improvements in efficacy with nutrient restriction (IC_{50} ratio) (Table 1). Factors such as the stoichiometry of inhibitor/channel interactions and resultant changes in the concentration dependence of channel block (Supplemental Fig. 2), compound stability in culture, and adsorption by serum may influence the magnitude of this ratio for individual compounds.

To explore therapeutic potential, we examined in vitro HeLa cell cytotoxicity. Several potent PSAC inhibitors were found to be nontoxic (Table 2), which suggests that they may be excellent starting points for medicinal chemical optimization to develop new antimalarial drugs that target parasite nutrient uptake.

Finally, we performed in vitro growth inhibition experiments with chloroquine, mefloquine, and artemisinin, approved antimalarial drugs that act at unrelated targets within intracellular parasites. Each of these drugs was modestly less active in PGIM than in standard medium (Table 1), providing evidence against nonspecific effects of our modified in vitro growth conditions. The improved efficacy of PSAC inhibitors with nutrient restriction is in contrast to the effect on existing antimalarial drugs and, therefore, implicates a distinct mechanism of action.

Discussion

Conservation of both PSAC activity and the recently implicated *clag3* genes in rodent, avian, and primate malaria species suggests that this ion channel serves an important role for the intracellular parasite. Because the channel is absent from other apicomplexan parasites and higher organisms (Alkhalil et al., 2007), inhibitors may be suitable starting points for the development of highly specific antimalarial drugs. The biological role of PSAC was unclear, however, and concerns that the channel might be only an epiphenomenon related to infection hampered progress toward therapeutic agents (Staines et al., 2007). Here, we addressed this uncertainty through studies with isolate-specific and broad-spectrum PSAC inhibitors, linkage analysis in a genetic cross, molecular studies, and in vitro selections. These studies provided experimental evidence for an essential and targetable role of PSAC in nutrient acquisition for the intracellular parasite.

Previous growth inhibition studies with PSAC inhibitors have reported discrepancies between the concentrations required for transport inhibition and those needed to inhibit in vitro parasite growth (Staines et al., 2004; Pillai et al., 2010). In light of our findings, this discrepancy likely results from the use of RPMI 1640 medium, which was designed with high concentrations of many nutrients to maximize the growth of diverse cell types. Our examination of individual substrates revealed that isoleucine uptake through PSAC serves an essential role for the parasite. Plasma isoleucine concentrations in developed countries range between 60 and 95 μM (Armstrong and Stave, 1973; Milsom et al., 1979), with values likely to be lower in malaria-endemic countries (Saunders et al., 1967). These measured values are significantly lower than the 381 μM in RPMI 1640 medium. Furthermore, dose-response studies suggest that PSAC-mediated uptake is rate-limiting at these physiological concentrations (Fig. 1A). Although glutamine and hypoxanthine dose-response studies did not show similar effects alone, their combined restriction to produce PGIM yielded further improvements in PSAC inhibitor efficacy. Future refinements of PGIM to include other permeant nutrients with high concentrations in RPMI 1640 medium may yield further improvements in in vitro PSAC inhibitor efficacy. Separate studies, such as in vivo efficacy studies with rodent malaria models, will be necessary to determine whether our findings can be translated into future antimalarial drugs.

Marked changes in inhibitor efficacy with relatively modest manipulations raise questions regarding the optimal conditions for high-throughput screens that use in vitro growth-inhibition assays to identify antimalarial drug leads; to date, such screens have used only standard RPMI 1640 medium (Plouffe et al., 2008; Gamo et al., 2010; Guiguemde et al., 2010). Although three existing antimalarial drugs exhibited unchanged efficacy with nutrient restriction (Table 1), it is important to recognize that in vitro parasite growth depends on many factors. We envision that compounds acting at some downstream sites involved in nutrient utilization or metabolism will also exhibit improved efficacy in more-physiological media such as PGIM. Such compounds might act synergistically with PSAC inhibitors. Future high-throughput screens that quantify parasite growth inhibition should consider the medium and other growth conditions carefully; conditions that most closely reproduce in vivo parasite development may be fruitful.

Although our studies provide additional evidence for the involvement of parasite *clag3* genes in PSAC activity, there are still fundamental questions regarding the composition and structure of this unusual ion channel (Desai, 2012). The results of prior studies of these genes are largely consistent with our findings (Kaneko et al., 2001; Cortés et al., 2007; Vincensini et al., 2008), but there are some interesting discrepancies with a study that reported a *clag3*-knockdown parasite (Comeaux et al., 2011). That study used DNA transfection to disrupt *clag3.2* and replace it with the selectable marker *hDHFR*; subsequent application of a dihydrofolate reductase inhibitor led to expression of *hDHFR* and silencing of *clag3.1*, presumably through the epigenetic mechanisms characterized here. Because both native *clag3* genes exhibited undetectable expression in that study, the findings con-

TABLE 2
HeLa cell cytotoxicity and specificity index for parasite killing

PSAC Inhibitor	HeLa Cell CC_{50}	Specificity (HeLa Cell CC_{50}/Parasite PGIM IC_{50})
	μM	
1	30	110
9	>100	>430
2	>100	>240
TP-52	>100	>530
5	>100	>50
ISG-21	86	43,000

CC_{50}, concentration of inhibitor that reduced conversion of MTS to formazan by 50%.

trast with the essential role in nutrient uptake proposed here. PSAC activity remains to be examined in the knockdown parasite; molecular studies are also required to explore ectopic recombination or other compensatory changes that might circumvent gene suppression (Fig. 4). Another possibility, i.e., that only some parasite lines require channel-mediated nutrient uptake, might reconcile our findings with the observation of a viable *clag3*-knockdown parasite. In that case, surveys of clinical isolates from patients with malaria might reveal novel PSAC-null parasite lines. Such studies should be pursued, because they are complementary to in vivo efficacy studies with rodent malaria species.

Allele-specific inhibitors, such as ISPA-28, represent useful reagents for examining epigenetic silencing mechanisms. In addition to the *clag3* genes, several other parasite gene families exhibit regulated expression and switching to increase antigenic diversity and to achieve immune evasion (Scherf et al., 1998; Lavazec et al., 2007; Mok et al., 2007; Deitsch et al., 2009). ISPA-28 is especially useful because it can be used in both positive and negative selections for the Dd2 *clag3.1* gene; our transport and growth inhibition strategies permit selection of channels that are either sensitive or resistant to this inhibitor. By combining these strategies, we identified a defect in *clag3* gene-switching in the Dd2 line; intact switching in the 7C20 parasite, which is isogenic at the chromosome 3 locus, excludes defects in *cis*-regulatory elements such as the promoter and instead suggests other determinants, possibly transcription factors (Tonkin et al., 2009). Our selections also show that Dd2 parasites can overcome this switching defect through ectopic recombination between the two *clag3* genes to produce a new chimeric gene. This chimeric gene is transcription-competent and encodes ISPA-28-resistant channels. Similar recombination events have been documented for other virulence genes within subtelomeric regions of the parasite genome (Kraemer and Smith, 2003); they likely account for the observed variations in *clag3* copy numbers for common laboratory parasite lines (Chung et al., 2007).

Our studies suggest that nutrient uptake at the host membrane is rate-limiting. Although the composition of PSAC and the precise in vivo role of the channel are poorly understood, our findings support continued pursuit of antimalarial drug discovery targeting this unusual ion channel. This target is especially attractive because some available PSAC inhibitors sterilize cultures at clinically achievable concentrations, with efficacies comparable to those of existing antimalarial drugs (Table 1). A legitimate concern relates to functional differences between channels of distinct parasite lines and associated polymorphisms in the *clag3* product (Alkhalil et al., 2004, 2009; Nguitragool et al., 2011). Will such variability reduce clinical effectiveness against malaria or speed drug resistance? We do not think so. Critical channel properties, such as the list of permeant solutes and their relative transport rates, are strictly conserved in *P. falciparum* and other malaria parasite species (Lisk and Desai, 2005). In parallel with this observation, informatic analyses of the *clag3* product revealed highly conserved domains separated by only a few polymorphic regions. In addition to sites that function in solute recognition and permeation, domains that function in trafficking, insertion, and regulation of the channel at the host erythrocyte surface may also be conserved and, therefore, targetable.

Acknowledgments

We dedicate this article to the memory of Ian Bathurst, the Medicines for Malaria Venture project director for these studies.

Authorship Contributions

Participated in research design: Pillai, Nguitragool, Lyko, Dolinta, Butler, Nguyen, Peet, Bowlin, and Desai.

Conducted experiments: Pillai, Nguitragool, Lyko, Dolinta, Butler, Nguyen, and Desai.

Performed data analysis: Pillai, Nguitragool, Lyko, Dolinta, Butler, Nguyen, Peet, Bowlin, and Desai.

Wrote or contributed to the writing of the manuscript: Pillai, Nguitragool, Lyko, Dolinta, Butler, Nguyen, Peet, Bowlin, and Desai.

References

Akkaya C, Shumilina E, Bobballa D, Brand VB, Mahmud H, Lang F, and Huber SM (2009) The *Plasmodium falciparum*-induced anion channel of human erythrocytes is an ATP-release pathway. *Pflugers Arch* **457:**1035–1047.

Alkhalil A, Cohn JV, Wagner MA, Cabrera JS, Rajapandi T, and Desai SA (2004) *Plasmodium falciparum* likely encodes the principal anion channel on infected human erythrocytes. *Blood* **104:**4279–4286.

Alkhalil A, Hill DA, and Desai SA (2007) Babesia and plasmodia increase host erythrocyte permeability through distinct mechanisms. *Cell Microbiol* **9:**851–860.

Alkhalil A, Hong L, Nguitragool W, and Desai SA (2012) Voltage-dependent inactivation of the plasmodial surface anion channel via a cleavable cytoplasmic component. *Biochim Biophys Acta* **1818:**367–374.

Alkhalil A, Pillai AD, Bokhari AA, Vaidya AB, and Desai SA (2009) Complex inheritance of the plasmodial surface anion channel in a *Plasmodium falciparum* genetic cross. *Mol Microbiol* **72:**459–469.

Armstrong MD and Stave U (1973) A study of plasma free amino acid levels. II. Normal values for children and adults. *Metabolism* **22:**561–569.

Asahi H, Kanazawa T, Kajihara Y, Takahashi K, and Takahashi T (1996) Hypoxanthine: a low molecular weight factor essential for growth of erythrocytic *Plasmodium falciparum* in a serum-free medium. *Parasitology* **113:**19–23.

Boddey JA, Hodder AN, Günther S, Gilson PR, Patsiouras H, Kapp EA, Pearce JA, de Koning-Ward TF, Simpson RJ, Crabb BS, et al. (2010) An aspartyl protease directs malaria effector proteins to the host cell. *Nature* **463:**627–631.

Brand VB, Sandu CD, Duranton C, Tanneur V, Lang KS, Huber SM, and Lang F (2003) Dependence of *Plasmodium falciparum* in vitro growth on the cation permeability of the human host erythrocyte. *Cell Physiol Biochem* **13:**347–356.

Broman KW, Wu H, Sen S, and Churchill GA (2003) R/qtl: QTL mapping in experimental crosses. *Bioinformatics* **19:**889–890.

Chung WY, Gardiner DL, Anderson KA, Hyland CA, Kemp DJ, and Trenholme KR (2007) The *CLAG/RhopH1* locus on chromosome 3 of *Plasmodium falciparum*: two genes or two alleles of the same gene? *Mol Biochem Parasitol* **151:**229–232.

Comeaux CA, Coleman BI, Bei AK, Whitehurst N, and Duraisingh MT (2011) Functional analysis of epigenetic regulation of tandem *RhopH1/clag* genes reveals a role in *Plasmodium falciparum* growth. *Mol Microbiol* **80:**378–390.

Cortés A, Carret C, Kaneko O, Yim Lim BY, Ivens A, and Holder AA (2007) Epigenetic silencing of *Plasmodium falciparum* genes linked to erythrocyte invasion. *PLoS Pathog* **3:**e107.

Deitsch KW, Lukehart SA, and Stringer JR (2009) Common strategies for antigenic variation by bacterial, fungal and protozoan pathogens. *Nat Rev Microbiol* **7:**493–503.

Desai SA (2012) Ion and nutrient uptake by malaria parasite-infected erythrocytes. *Cell Microbiol* **14:**1003–1009.

Desai SA, Bezrukov SM, and Zimmerberg J (2000) A voltage-dependent channel involved in nutrient uptake by red blood cells infected with the malaria parasite. *Nature* **406:**1001–1005.

Freitas-Junior LH, Bottius E, Pirrit LA, Deitsch KW, Scheidig C, Guinet F, Nehrbass U, Wellems TE, and Scherf A (2000) Frequent ectopic recombination of virulence factor genes in telomeric chromosome clusters of *P. falciparum*. *Nature* **407:**1018–1022.

Gamo FJ, Sanz LM, Vidal J, de Cozar C, Alvarez E, Lavandera JL, Vanderwall DE, Green DV, Kumar V, Hasan S, et al. (2010) Thousands of chemical starting points for antimalarial lead identification. *Nature* **465:**305–310.

Gero AM and Wood AM (1991) New nucleoside transport pathways induced in the host erythrocyte membrane of malaria and *Babesia* infected cells. *Adv Exp Med Biol* **309A:**169–172.

Ginsburg H, Krugliak M, Eidelman O, and Cabantchik ZI (1983) New permeability pathways induced in membranes of *Plasmodium falciparum* infected erythrocytes. *Mol Biochem Parasitol* **8:**177–190.

Ginsburg H, Kutner S, Krugliak M, and Cabantchik ZI (1985) Characterization of permeation pathways appearing in the host membrane of *Plasmodium falciparum* infected red blood cells. *Mol Biochem Parasitol* **14:**313–322.

Guiguemde WA, Shelat AA, Bouck D, Duffy S, Crowther GJ, Davis PH, Smithson DC, Connelly M, Clark J, Zhu F, et al. (2010) Chemical genetics of *Plasmodium falciparum*. *Nature* **465:**311–315.

Hill DA, Pillai AD, Nawaz F, Hayton K, Doan L, Lisk G, and Desai SA (2007) A blasticidin S-resistant *Plasmodium falciparum* mutant with a defective plasmodial surface anion channel. *Proc Natl Acad Sci USA* **104:**1063–1068.

Homewood CA and Neame KD (1974) Malaria and the permeability of the host erythrocyte. *Nature* **252:**718–719.

Istvan ES, Dharia NV, Bopp SE, Gluzman I, Winzeler EA, and Goldberg DE (2011)

Validation of isoleucine utilization targets in *Plasmodium falciparum*. *Proc Natl Acad Sci USA* **108:**1627–1632.
Kaneko O, Tsuboi T, Ling IT, Howell S, Shirano M, Tachibana M, Cao YM, Holder AA, and Torii M (2001) The high molecular mass rhoptry protein, RhopH1, is encoded by members of the *clag* multigene family in *Plasmodium falciparum* and *Plasmodium yoelii*. *Mol Biochem Parasitol* **118:**223–231.
Kirk K, Horner HA, Elford BC, Ellory JC, and Newbold CI (1994) Transport of diverse substrates into malaria-infected erythrocytes via a pathway showing functional characteristics of a chloride channel. *J Biol Chem* **269:**3339–3347.
Kraemer SM and Smith JD (2003) Evidence for the importance of genetic structuring to the structural and functional specialization of the *Plasmodium falciparum* var gene family. *Mol Microbiol* **50:**1527–1538.
Kutner S, Breuer WV, Ginsburg H, and Cabantchik ZI (1987) On the mode of action of phlorizin as an antimalarial agent in in vitro cultures of *Plasmodium falciparum*. *Biochem Pharmacol* **36:**123–129.
Lavazec C, Sanyal S, and Templeton TJ (2007) Expression switching in the stevor and Pfmc-2TM superfamilies in *Plasmodium falciparum*. *Mol Microbiol* **64:**1621–1634.
Lew VL, Macdonald L, Ginsburg H, Krugliak M, and Tiffert T (2004) Excess haemoglobin digestion by malaria parasites: a strategy to prevent premature host cell lysis. *Blood Cells Mol Dis* **32:**353–359.
Lisk G and Desai SA (2005) The plasmodial surface anion channel is functionally conserved in divergent malaria parasites. *Eukaryot Cell* **4:**2153–2159.
Lisk G, Kang M, Cohn JV, and Desai SA (2006) Specific inhibition of the plasmodial surface anion channel by dantrolene. *Eukaryot Cell* **5:**1882–1893.
Lisk G, Pain M, Gluzman IY, Kambhampati S, Furuya T, Su XZ, Fay MP, Goldberg DE, and Desai SA (2008) Changes in the plasmodial surface anion channel reduce leupeptin uptake and can confer drug resistance in *P. falciparum*-infected erythrocytes. *Antimicrob Agents Chemother* **52:**2346–2354.
Liu J, Istvan ES, Gluzman IY, Gross J, and Goldberg DE (2006) *Plasmodium falciparum* ensures its amino acid supply with multiple acquisition pathways and redundant proteolytic enzyme systems. *Proc Natl Acad Sci USA* **103:**8840–8845.
Lyko B, Hammershaimb EA, Nguitragool W, Wellems TE, and Desai SA (2012) A high-throughput method to detect *Plasmodium falciparum* clones in limiting dilution microplates. *Malar J* **11:**124.
Marshall NJ, Goodwin CJ, and Holt SJ (1995) A critical assessment of the use of microculture tetrazolium assays to measure cell growth and function. *Growth Regul* **5:**69–84.
Martin RE and Kirk K (2007) Transport of the essential nutrient isoleucine in human erythrocytes infected with the malaria parasite *Plasmodium falciparum*. *Blood* **109:**2217–2224.
Matsuhisa S, Takesawa S, and Sakai K (1987) Binary-solute adsorption of dosed drugs on serum-albumin. *Chem Eng J Biochem Eng J* **34:**B21–B27.
Milsom JP, Morgan MY, and Sherlock S (1979) Factors affecting plasma amino acid concentrations in control subjects. *Metabolism* **28:**313–319.
Mok BW, Ribacke U, Winter G, Yip BH, Tan CS, Fernandez V, Chen Q, Nilsson P, and Wahlgren M (2007) Comparative transcriptomal analysis of isogenic *Plasmodium falciparum* clones of distinct antigenic and adhesive phenotypes. *Mol Biochem Parasitol* **151:**184–192.
Nguitragool W, Bokhari AA, Pillai AD, Rayavara K, Sharma P, Turpin B, Aravind L, and Desai SA (2011) Malaria parasite *clag3* genes determine channel-mediated nutrient uptake by infected red blood cells. *Cell* **145:**665–677.
Pillai AD, Pain M, Solomon T, Bokhari AA, and Desai SA (2010) A cell-based high-throughput screen validates the plasmodial surface anion channel as an antimalarial target. *Mol Pharmacol* **77:**724–733.
Plouffe D, Brinker A, McNamara C, Henson K, Kato N, Kuhen K, Nagle A, Adrián F, Matzen JT, Anderson P, et al. (2008) In silico activity profiling reveals the mechanism of action of antimalarials discovered in a high-throughput screen. *Proc Natl Acad Sci USA* **105:**9059–9064.
Quashie NB, Ranford-Cartwright LC, and de Koning HP (2010) Uptake of purines in *Plasmodium falciparum*-infected human erythrocytes is mostly mediated by the human equilibrative nucleoside transporter and the human facilitative nucleobase transporter. *Malar J* **9:**36.
Russo I, Babbitt S, Muralidharan V, Butler T, Oksman A, and Goldberg DE (2010) Plasmepsin V licenses *Plasmodium* proteins for export into the host erythrocyte. *Nature* **463:**632–636.
Saliba KJ, Horner HA, and Kirk K (1998) Transport and metabolism of the essential vitamin pantothenic acid in human erythrocytes infected with the malaria parasite *Plasmodium falciparum*. *J Biol Chem* **273:**10190–10195.
Sato JD and Kan M (2001) Media for culture of mammalian cells. *Curr Protoc Cell Biol* Unit 1.2.
Saunders SJ, Truswell AS, Barbezat GO, Wittman W, and Hansen JD (1967) Plasma free aminoacid pattern in protein-calorie malnutrition: reappraisal of its diagnostic value. *Lancet* **2:**795–797.
Scherf A, Hernandez-Rivas R, Buffet P, Bottius E, Benatar C, Pouvelle B, Gysin J, and Lanzer M (1998) Antigenic variation in malaria: in situ switching, relaxed and mutually exclusive transcription of *var* genes during intra-erythrocytic development in *Plasmodium falciparum*. *EMBO J* **17:**5418–5426.
Scherf A, Lopez-Rubio JJ, and Riviere L (2008) Antigenic variation in *Plasmodium falciparum*. *Annu Rev Microbiol* **62:**445–470.
Staines HM, Alkhalil A, Allen RJ, De Jonge HR, Derbyshire E, Egée S, Ginsburg H, Hill DA, Huber SM, Kirk K, et al. (2007) Electrophysiological studies of malaria parasite-infected erythrocytes: current status. *Int J Parasitol* **37:**475–482.
Staines HM, Dee BC, O'Brien M, Lang HJ, Englert H, Horner HA, Ellory JC, and Kirk K (2004) Furosemide analogues as potent inhibitors of the new permeability pathways of *Plasmodium falciparum*-infected human erythrocytes. *Mol Biochem Parasitol* **133:**315–318.
Staines HM, Ellory JC, and Kirk K (2001) Perturbation of the pump-leak balance for Na^+ and K^+ in malaria-infected erythrocytes. *Am J Physiol Cell Physiol* **280:**C1576–C1587.
Tamez PA, Bhattacharjee S, van Ooij C, Hiller NL, Llinás M, Balu B, Adams JH, and Haldar K (2008) An erythrocyte vesicle protein exported by the malaria parasite promotes tubovesicular lipid import from the host cell surface. *PLoS Pathog* **4:**e1000118.
Tonkin CJ, Carret CK, Duraisingh MT, Voss TS, Ralph SA, Hommel M, Duffy MF, Silva LM, Scherf A, Ivens A, et al. (2009) Sir2 paralogues cooperate to regulate virulence genes and antigenic variation in *Plasmodium falciparum*. *PLoS Biol* **7:**e84.
Vincensini L, Fall G, Berry L, Blisnick T, and Braun Breton C (2008) The RhopH complex is transferred to the host cell cytoplasm following red blood cell invasion by *Plasmodium falciparum*. *Mol Biochem Parasitol* **160:**81–89.
Wellems TE, Panton LJ, Gluzman IY, do Rosario VE, Gwadz RW, Walker-Jonah A, and Krogstad DJ (1990) Chloroquine resistance not linked to *mdr*-like genes in a *Plasmodium falciparum* cross. *Nature* **345:**253–255.
Winterberg M, Rajendran E, Baumeister S, Bietz S, Kirk K, and Lingelbach K (2012) Chemical activation of a high-affinity glutamate transporter in human erythrocytes and its implications for malaria-parasite-induced glutamate uptake. *Blood* **119:**3604–3612.

Address correspondence to: Dr. Sanjay A. Desai, Laboratory of Malaria and Vector Research, National Institute of Allergy and Infectious Diseases, National Institutes of Health, 12735 Twinbrook Parkway, Room 3W-01, Rockville, MD 20852. E-mail: sdesai@niaid.nih.gov